

# Associated 21-cm HI absorption towards the radio galaxy 3C 452 (J2245+3941)

Neeraj Gupta\* and D.J. Saikia

*National Centre for Radio Astrophysics, TIFR, Pune 411 007, India*

Accepted. Received; in original form

## ABSTRACT

We report the detection of 21-cm HI absorption towards the core of the Fanaroff-Riley II radio galaxy 3C 452 (J2245+3941). The absorption profile is well resolved into three components; the strongest and narrowest component being coincident with the velocity corresponding to [O III] emission lines while the other two components are blue-shifted with respect to it by  $\sim 30$  and  $\sim 115$   $\text{km s}^{-1}$ . If the systemic velocity of the host galaxy is determined from low-ionization lines, which are red-shifted with respect to the [O III] doublet by about  $\sim 200$   $\text{km s}^{-1}$ , then both the [O III] emission and 21-cm absorption lines are associated with outflowing material. The neutral hydrogen column density is estimated to be  $N(\text{HI}) = 6.39 \times 10^{20} (T_s/100)(f_c/1.0)^{-1} \text{ cm}^{-2}$ , where  $T_s$  and  $f_c$  are the spin temperature and partial coverage of the background source respectively. If the 21-cm absorber is also responsible for the nuclear extinction at infrared wavelengths and x-ray absorption, then for a spin temperature of  $\sim 8000$  K, the absorber occults only  $\sim 10$  per cent of the radio core.

**Key words:** galaxies: active – galaxies: evolution – galaxies: nuclei – galaxies: absorption lines – radio lines: galaxies – galaxies: individual: 3C 452

## 1 INTRODUCTION

An understanding of the properties of the gaseous environments of radio galaxies and quasars could provide valuable insights towards understanding the phenomenon of radio activity associated with these objects and their evolution. Such studies also enable us to test consistency of these properties with the unified schemes for these objects. An important way of probing the neutral component of this gas over a wide range of length scales is via 21-cm HI absorption towards radio sources of different sizes. These range from the sub-galactic sized compact steep-spectrum (CSS) and gigahertz peaked-spectrum (GPS) sources, which are believed to be young ( $< 10^5$  yr), as compared with the larger sources which could extend to over a Mpc and are typically  $\sim 10^8$  yr old.

HI absorption lines are seen more often towards CSS and GPS objects, with the HI column densities being anticorrelated with the source sizes. The absorption profiles exhibit a variety of line profiles, suggesting complex gas motions (Vermeulen et al. 2003; Pihlström, Conway & Vermeulen 2003; Gupta et al. 2006). Gupta & Saikia (2006) have examined whether the HI column density is consistent with the unified scheme for radio galaxies and quasars by using core promi-

nence as an indicator of the orientation of the jet axis to the line of sight for a sample of 32 CSS and GPS objects. They find the relationship between the HI column density and core prominence to be consistent with the unified scheme in a paradigm where the HI gas is distributed in a circumnuclear disk with a scale smaller than the size of the compact radio sources. Very Long Baseline Interferometry (VLBI)-scale spectroscopic observations towards several sources such as the CSS object J0119+3210 (4C+31.04) and the cores of larger sources such as the well known Fanaroff-Riley class II (FR II) source Cyg A and the FRI objects NGC 4621 and Hydra A show evidence of absorption arising from a circumnuclear disk-like structure (Conway & Blanco 1995; Taylor 1996; Conway 1999; van Langevelde et al. 2000). Morganti et al. (2001) have suggested that there may be differences in the torus/disk between FRI and FR II sources, with those in FR Is being geometrically thin.

Compared with 21-cm absorption searches towards CSS and GPS sources the extended radio galaxies have received relatively less attention. Notable exceptions to this are the studies by van Gorkom et al. (1989) and Morganti et al. (2001) whose samples also contained larger radio sources in addition to the subgalactic-sized compact ones. To investigate whether the circumnuclear gas evolves as the source grows from CSS and GPS scales to the large radio sources, one needs to probe the distribution and properties of this

\* E-mail: neeraj@ncra.tifr.res.in (NG); djs@ncra.tifr.res.in (DJS)

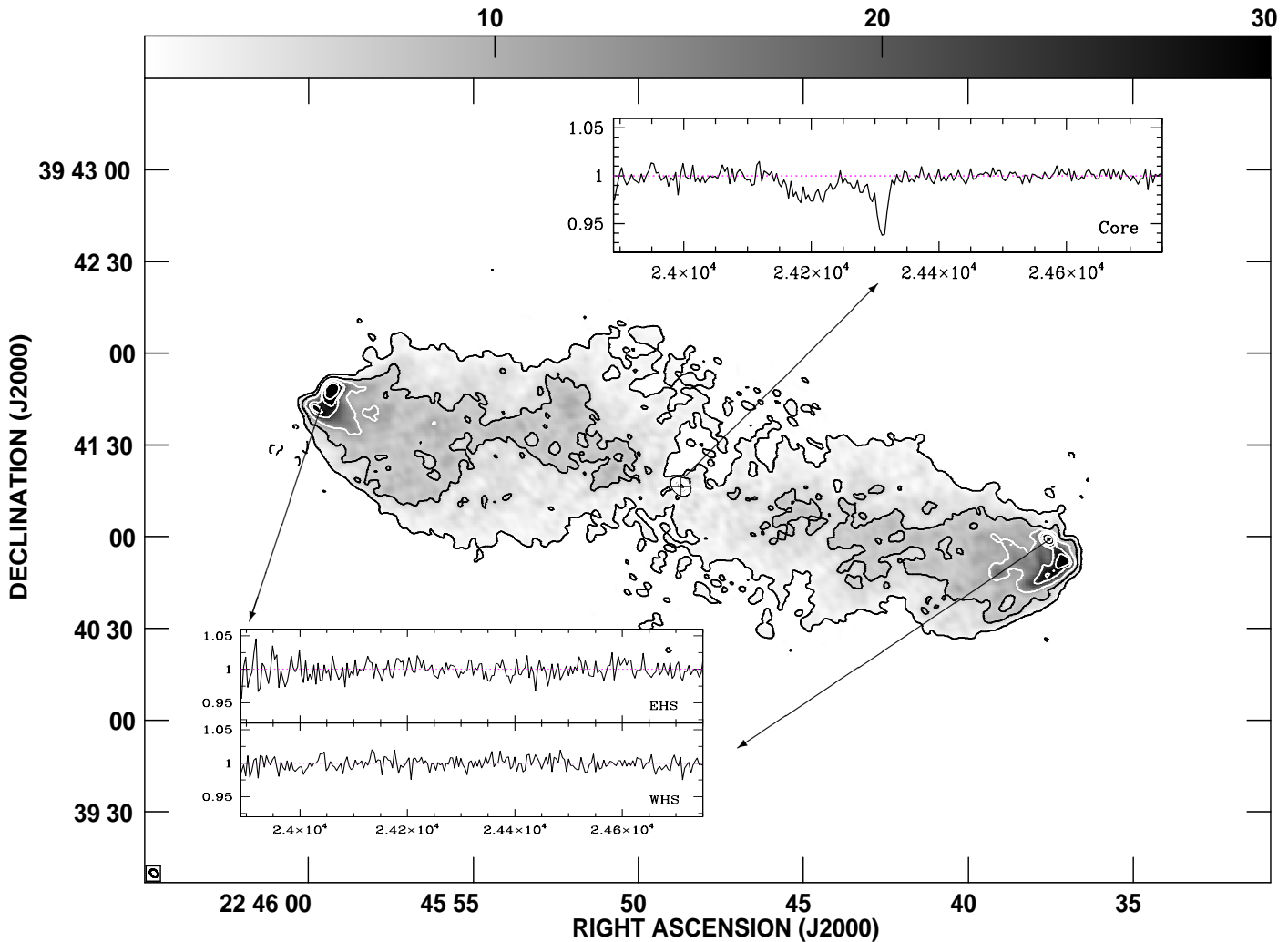


**Figure 1.** GMRT image of 3C 452 with an rms noise of 0.3 mJy/beam. The contour levels are  $1.5 \times (-2, -1, 1, 4, 8, 16, 20, 32, 64, 128)$  mJy/beam. The restoring beam of  $3.14'' \times 2.25''$  along position angle  $52^\circ$  is shown as an ellipse and the position of the optical host galaxy is marked with a cross. The spectra at the peak intensity pixel in the eastern hotspot (EHS), core and western hotspot (WHS) are also shown. For these x-axis and y-axis are heliocentric velocity in  $\text{km s}^{-1}$  and normalised intensity respectively.

gas on similar scales with comparable sensitivities. This can be achieved via 21-cm absorption measurements towards the compact cores of the large objects using high-resolution observations where the core is clearly resolved from the more extended bridge emission. Such observations will also help clarify any differences between FR I and FR II sources. However, very few such measurements exist in the literature. Amongst large FR II radio galaxies, two notable detections are Cyg A and 3C 353 (Conway & Blanco 1995; Morganti et al. 2001). In this paper, we report the discovery of 21-cm absorption towards the core of the FR II radio galaxy 3C 452 with the Giant Metrewave Radio Telescope (GMRT), and examine the properties of this 21-cm absorber in the light of observations at other wavelengths.

## 2 3C 452 (J2245+3941)

3C 452 is a high-excitation narrow-line FR II radio galaxy at the redshift,  $z_{em}=0.08110$  determined using the

[O III]  $\lambda\lambda 4959, 5007 \text{ \AA}$  emission lines (Lawrence et al. 1996; Jackson & Rawlings 1997). This is consistent with the estimate from the  $H\beta$  line within  $\sim 30 \text{ km s}^{-1}$ . However from the data of Lawrence et al. we find that the low-ionization forbidden emission lines namely, [O I], [O II], [N II] and [S II] are all systematically red-shifted with respect to it by  $\sim 200 \text{ km s}^{-1}$ . Further, the low-ionization lines appear broader (FWHM  $\sim 900 \text{ km s}^{-1}$ ) than the high-ionization ones which have a FWHM of  $\sim 600 \text{ km s}^{-1}$ , suggesting that the low-ionization lines may be arising from shock-ionised gas (see Villar-Martin et al. 1999). The total radio luminosity of 3C 452 at 5 GHz is  $3.6 \times 10^{25} \text{ W Hz}^{-1} \text{ sr}^{-1}$  ( $H_0=71 \text{ km s}^{-1} \text{ Mpc}^{-1}$ ,  $\Omega_m=0.27$ ,  $\Omega_\Lambda=0.73$ ; Spergel et al. 2003), which is well above the dividing line for the two FR types. At radio wavelengths the source exhibits a symmetric triple morphology with a largest angular size of 256 arcsec, which corresponds to a linear size of 386 kpc (e.g. Black et al. 1992; Dennett-Thorpe et al. 1999). The compact arcsec-scale radio core is resolved with an angular resolution of  $\sim 1.2 \text{ mas}$  into a central peak of emission, which we call the ‘nucleus’, and

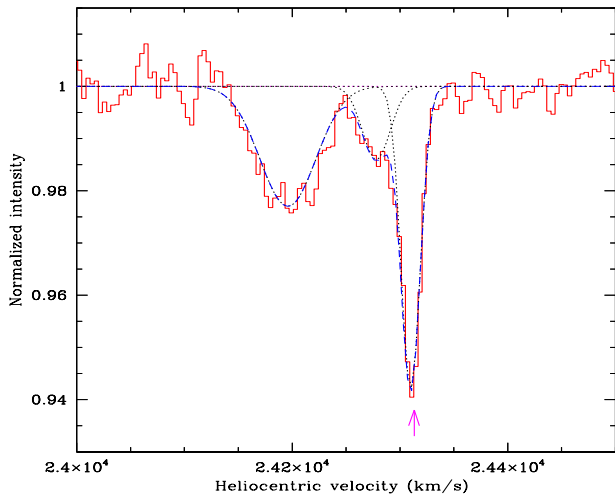


**Figure 2.** The HI absorption spectrum (histogram) towards the core of the radio galaxy 3C 452. The spectrum has been smoothed using a 3-pixel wide boxcar filter. The three Gaussian components fitted to the absorption profile and the sum of these components i.e. the fit are plotted as dotted and dashed lines respectively. The systemic velocity ( $24313 \text{ km s}^{-1}$ ) determined using [O III] emission lines has been marked by an arrow.

symmetric jet-like structures on opposite sides of it (Giovannini et al. 2001). Most of the emission is within  $\sim 5 \text{ mas}$  ( $7.6 \text{ pc}$ ) of the radio nucleus, although faint emission is seen extending upto  $\sim 20 \text{ mas}$  ( $30 \text{ pc}$ ) from the radio nucleus on both sides. Using the jet symmetry and core prominence at  $5 \text{ GHz}$ , Giovannini et al. suggest that this source must be oriented at an angle greater than  $\sim 60^\circ$  to the line of sight. The core as well as diffuse emission associated with the lobes have been detected in x-rays using the Chandra telescope (Isobe et al. 2002). The HST WFPC-2 image of the host galaxy suggests the presence of a faint dust lane roughly perpendicular to the radio axis of the source (de Koff et al. 2000).

### 3 OBSERVATIONS AND DATA ANALYSES

We observed 3C 452 with the GMRT to search for associated 21-cm absorption towards the radio source. 3C 452 was observed on 2005 Dec 11 with a bandwidth of  $4 \text{ MHz}$  for  $\sim 9$  hours. In these observations we made use of the new high-resolution mode of the GMRT correlator software. This allows one to split the baseband bandwidth into 256 channels, instead of the usual 128 channels. This provided us a spectral resolution of  $\sim 3.6 \text{ km s}^{-1}$ . The local oscillator chain and FX correlator system were tuned to centre the baseband bandwidth at  $1313.85 \text{ MHz}$ , the redshifted 21-cm frequency corresponding to  $z_{em}=0.0811$ . We observed standard flux density calibrators 3C 286 and 3C 48 every 3 hours to correct for the variations in amplitudes and bandpass. The compact radio source J2202+4216 was also observed approximately every 35 minutes for phase calibration of the array. A total of  $\sim 5.6$  hours of data on source were acquired in both the circular polarization channels RR and LL.

The data were reduced in the standard way using As-

**Table 1.** Observational results

Component	Peak flux Jy/b	$\sigma$ mJy/b	$\tau_{1\sigma}$ $10^{-3}$	$N(\text{HI})$ $10^{19} \text{ cm}^{-2}$
EHS	0.094	1.1	$<11.7$	$<13.6$
Core*	0.194	1.0	—	—
WHS	0.128	1.1	$<8.59$	$<9.95$

Col. 1: radio component; col. 2: peak flux density; col. 3: rms noise in the spectrum; col. 4: optical depth estimate and col. 5: HI column density or  $3\sigma$  upper limit to it.  $T_s=100 \text{ K}$  and  $\Delta v=20 \text{ km s}^{-1}$  have been adopted for estimating  $N(\text{HI})$  upper limits.

\* See Table 2.

**Table 2.** Multiple Gaussian fit to the HI absorption spectrum

Id. no.	$v_{\text{hel}}$ $\text{km s}^{-1}$	FWHM $\text{km s}^{-1}$	Frac. abs.	$N(\text{HI})$ $10^{20} \left(\frac{T_s}{100}\right) \left(\frac{f_c}{1.0}\right)^{-1}$ $\text{cm}^{-2}$
1	24196	61(3)	0.023(0.001)	2.71
2	24278	31(4)	0.014(0.002)	0.84
3	24310	21(1)	0.058(0.002)	2.35

tronomical Image Processing System (AIPS) package. After the initial flagging or editing of bad data and calibration, source and calibrator data were examined for baselines and timestamps affected by Radio Frequency Interference (RFI). These data were excluded from further analysis. A continuum image of the source was made using calibrated data averaged over 60 line-free channels. Due to our interest in absorption towards compact components like the core, the imaging was done without any  $uv$  cut-off or tapering in the visibility plane. This provided us with the highest possible resolution. This image was then self-calibrated until a satisfactory map was obtained (see Fig. 1). The self-calibration complex gains determined from this were applied to all the 256 frequency channels and continuum emission was subtracted from this visibility data cube using the same map. Spectra at various positions on the radio galaxy 3C 452 were extracted from this cube. The whole process was done separately for Stokes RR and LL to check for consistency. The two polarization channels were then combined to get the final Stokes I spectrum, which was then shifted to the heliocentric frame.

### 4 RESULTS AND DISCUSSION

In Fig. 1 we present our GMRT image of 3C 452 at  $1313 \text{ MHz}$ , which shows the radio core, the symmetrically located hotspots on opposite sides of the parent optical galaxy and the extended bridge of emission. The peak flux density of the radio core in our image is  $194 \text{ mJy/beam}$ . The peak intensities for the brightest components in the eastern and western lobes, referred to as the eastern hotspot (EHS) and the western hotspot (WHS) are given in Table. 1. The total flux density in the image is  $9.98 \text{ Jy}$  at  $1313 \text{ MHz}$ , which is within a few per cent of the value of  $10.2 \text{ Jy}$ . The latter has been estimated using the measurements with least errors at  $750$  and  $4850 \text{ MHz}$  from the NASA Extragalactic Database.

The HI absorption spectra towards the core and hotspots of 3C 452 are presented in Fig. 1. HI absorption has been detected clearly towards the core of the radio galaxy while no absorption has been detected towards the hotspots or any other part of the source. The rms noise in the spectra and  $1\text{-}\sigma$  upper limits to the optical depth towards EHS and WHS are presented in Table. 1. The HI column density,  $N(\text{HI})$ , integrated over the entire spectrum using the relation

$$N(\text{HI}) = 1.835 \times 10^{18} \frac{T_s \int \tau(v) dv}{f_c} \text{ cm}^{-2}, \quad (1)$$

where  $T_s$ ,  $\tau$  and  $f_c$  are the spin temperature, optical depth at a velocity  $v$  and the fraction of background emission covered by the absorber respectively, is  $6.39 \times 10^{20} (T_s/100)(1.0/f_c) \text{ cm}^{-2}$ . The absorption profile is well fitted with three Gaussian components (Fig. 2). The best fit parameters are summarised in Table 2. It may be noted that the widths of the components and corresponding column densities are typical of those observed in our Galaxy (e.g. Ferrière 2001; Dickey & Lockman 1990). The absorption profile consists of a strong narrow component near the velocity of the galaxy estimated from the [O III] emission lines and two broader components blue-shifted with respect to it by about  $\sim 30$  and  $\sim 115 \text{ km s}^{-1}$ . However different velocities for the host galaxy estimated from different emission lines can sometimes make it difficult to ascertain the kinematics of the absorbing gas (see e.g. Tadhunter et al. 2001; Vermeulen et al. 2006). In 3C 452 the velocity corresponding to the low-ionization lines would imply that the narrow and two broad 21-cm absorption lines are blue-shifted by  $\sim 200$ ,  $230$  and  $315 \text{ km s}^{-1}$ . This would then imply that both the [O III] emission and 21-cm absorption lines are associated with outflowing gas. Fast and broad outflows in HI with velocities extending up to several thousand  $\text{km s}^{-1}$  have been reported for a number of radio galaxies (Morganti, Tadhunter & Oosterloo 2005).

Amongst the two notable detections of 21-cm absorption towards the cores of extended FR II radio galaxies, namely Cyg A and 3C 353, the system associated with the narrow-line radio galaxy Cyg A has a FWHM of  $\sim 270 \text{ km s}^{-1}$  and column density of  $2.54 \times 10^{21} (T_s/100)(1.0/f_c) \text{ cm}^{-2}$  (Conway & Blanco 1995). The redshift of Cyg A determined from the [O III] emission lines is  $z_{em} = 0.05606$  (see Section 4.3 of Tadhunter et al. 2003). The 21-cm absorption line associated with it consists of two components; the narrower (FWHM  $\sim 102 \text{ km s}^{-1}$ ) and weaker one being consistent with the  $z_{em}$  while the other one (FWHM  $\sim 151 \text{ km s}^{-1}$ ) is red-shifted with respect to it by  $\sim 170 \text{ km s}^{-1}$ . In the weak-line radio galaxy 3C 353, the absorption-line (FWHM  $\sim 300 \text{ km s}^{-1}$ ) corresponds to a total HI column density of  $4.2 \times 10^{21} (T_s/100)(1.0/f_c) \text{ cm}^{-2}$  (Morganti et al. 2001). The peak of absorption is blue-shifted with respect to the systemic velocity of the host galaxy estimated from the [O III] and  $\text{H}\alpha$  emission lines by  $\sim 100 \text{ km s}^{-1}$ . Thus 21-cm absorption-line systems detected towards the cores of Cyg A, 3C 353 and 3C 452 have peaks of absorption red-shifted, blue-shifted and consistent with respect to the velocity corresponding to the [O III] emission line. Thus the absorption profiles are often complex suggesting radial motions (i.e infall or outflow) in addition to disks, as has been inferred for the CSS and GPS objects.

It is interesting to note that the low-ionization forbid-

den emission lines in 3C 452 are found to be broader and more red-shifted than the high-ionization ones. The low-ionization lines could then correspond to gas interacting with the jet, thereby being broadened. In that case, a plausible scenario to explain the different 21-cm absorption components is one in which [O III] emission lines represent the systemic velocity and the narrowest 21-cm absorption line component coincident with it, arises from gas in a circumnuclear disk aligned with the dust lane perpendicular to the radio source axis of 3C 452 (de Koff et al. 2000). The possibility of absorption occurring in such disks is consistent with a number of observational trends. For example, Morganti et al. (2001) detect 21-cm absorption towards 3 out of 4 narrow-line radio galaxies, while no absorption was detected towards 4 broad-line radio galaxies. The latter are expected to be inclined at smaller angles to the line of sight so that the disk is unlikely to produce significant HI absorption. These results of Morganti et al. are also consistent with the higher detection rate of 21-cm HI absorption towards radio galaxies compared with quasars (Vermeulen et al. 2003; Gupta et al. 2006). Gupta & Saikia (2006) for a sample of CSS and GPS sources find the dependence of  $N(\text{HI})$  on the degree of core prominence to be consistent with the HI having a disk-like distribution, with the source sizes being larger than the scale size of the disk. Thus, if we attribute the narrow component to be due to absorption by a disk, the broader blue-shifted components could still be due to outflowing gas.

In the following we compare our results with observations at infrared and x-ray wavelengths to constrain some of the properties of the absorbing material. The nuclear extinction of 3C 452 as measured by near-infrared observations is  $A_V > 2.30$  (Marchesini, Capetti & Celotti 2005). For the diffuse ISM of our Galaxy, the mean ratio of total neutral hydrogen i.e.  $N(\text{HI} + \text{H}_2)$  is related to visual extinction as

$$N(\text{HI} + \text{H}_2) = 1.89 \times 10^{21} A_V \text{ mag}^{-1} \text{ cm}^{-2} \quad (2)$$

(Bohlin, Savage & Drake 1978; Cardelli, Clayton & Mathis 1989). Using this relation and assuming that all the gas producing extinction is atomic we get for 3C 452,  $N(\text{HI}) > 2.2 \times 10^{21} \text{ cm}^{-2}$ . Its comparison with the total neutral hydrogen column density determined from 21-cm absorption implies  $T_s > 350 \text{ K}$  for  $f_c = 1.0$ . In fact, the spin temperature of 21-cm absorbing gas can be much higher than  $\sim 350 \text{ K}$ . For the warm neutral medium seen in the Galaxy  $T_s$  ranges from  $5000\text{--}8000 \text{ K}$  (Kulkarni & Heiles 1988). Such high spin temperatures are also expected to arise in the proximity of the active nucleus (Bahcall & Ekers 1969).

Using the Chandra telescope, Isobe et al. (2002) detected x-ray emission associated with the core and lobes of the radio galaxy. They infer that a total hydrogen column density  $N(\text{H}) \approx 6 \times 10^{23} \text{ cm}^{-2}$  is required to fit the x-ray spectrum towards the core. Even for a spin temperature of  $\sim 8000 \text{ K}$ , the 21-cm absorbing gas has at least an order of magnitude lesser column density than that required for x-ray absorption. This either implies that the x-ray absorbing gas is different from that responsible for 21-cm absorption or that the 21-cm absorber does not cover the core completely. The nucleus in the 5-GHz VLBI map of Giovannini et al. (2001) has a flux density of only  $\sim 20 \text{ mJy}$ . Assuming a spectral index of 0, this would then correspond to  $f_c \sim 0.1$ . Thus a spin temperature of  $\sim 8000 \text{ K}$  and  $f_c$  of  $\sim 0.1$  are

required if the gas producing 21-cm absorption and nuclear extinction also causes the x-ray absorption. It is worth mentioning here that reconciliation of x-ray absorbing column density with the absorbers detected at other wavelengths in AGN is a recurring problem (see e.g. Hamann 1997; Gallimore et al. 1999). In the simplest explanation the x-ray absorber and the UV or 21-cm absorption line systems are not cospatial. For example, in a 21-cm absorption study of a sample of 13 Seyfert galaxies, Gallimore et al. (1999) did not find any correlation between the 21-cm and x-ray absorbing column density. The nuclear extinction measured for a complete sub-sample of 3CR radio sources, which includes 3C 452, ranges from 0 to 9 mag (Marchesini et al. 2004). Adopting 9 mag as an upper limit on  $A_V$  for 3C 452 and  $f_c=1.0$  for the 21-cm absorber would then imply that the gas producing 21-cm absorption and nuclear extinction, and x-ray absorption are not cospatial. HI observations via VLBI techniques are required to constrain the properties and location of the absorbing clouds and further investigate this scenario. The x-ray spectrum of diffuse emission associated with the lobes is consistent with the Galactic value of  $N(\text{H})=1.2 \times 10^{21} \text{ cm}^{-2}$ . This is consistent with the limits on the neutral hydrogen column density derived from the GMRT spectra towards the radio hotspots (Table 1).

## 5 SUMMARY

We have reported the detection of 21-cm absorption towards the core of the FR II radio galaxy 3C 452. The absorption profile is resolved into three components. The deepest and narrowest of these is consistent with the velocity corresponding to [O III] emission lines. The other two broader components are blue-shifted with respect to it by  $\sim 30$  and  $\sim 115 \text{ km s}^{-1}$ . If the systemic velocity of the host galaxy is determined from low-ionization forbidden emission lines then both the [O III] emission and 21-cm absorption lines are associated with outflowing material. The 21-cm components are blue-shifted relative to the low-ionization lines by  $\sim 200$ , 230 and  $315 \text{ km s}^{-1}$  respectively. The neutral hydrogen column density of the gas is estimated to be  $N(\text{HI})=6.39 \times 10^{20} (T_s/100)(f_c/1.0)^{-1} \text{ cm}^{-2}$ . If the 21-cm absorber is also responsible for the nuclear absorption seen at x-ray wavelengths, then for a spin temperature of  $\sim 8000 \text{ K}$ , the absorber occults only  $\sim 10$  per cent of the radio core. This would also be consistent with the nuclear extinction seen at infrared wavelengths. In our GMRT spectrum we do not detect 21-cm absorption towards locations other than the radio core of 3C 452. The upper limit on  $N(\text{HI})$  derived from spectra towards the hotspots is consistent with constraints on  $N(\text{H})$  obtained from the diffuse x-ray emission associated with the radio lobes.

## ACKNOWLEDGMENTS

We thank Raffaella Morganti, the referee, and Raghunathan Srikanth for many useful suggestions and comments. We also thank the numerous contributors to the GNU/Linux group. This research has made use of the NASA/IPAC Extragalactic Database (NED) which is operated by the Jet Propulsion Laboratory, California Institute of Technology,

under contract with the National Aeronautics and Space Administration. We thank the staff of GMRT for their assistance during our observations. The GMRT is a national facility operated by the National Centre for Radio Astrophysics of the Tata Institute of Fundamental Research.

## REFERENCES

- Bahcall J.N., Ekers R.D., 1969, ApJ, 157, 1055  
 Black A.R.S., Baum S.A., Leahy J.P., Perley R.A., Riley J.M., Scheuer P.A.G., 1992, MNRAS, 256, 186  
 Bohlin R.C., Savage B.D., Drake J.F., 1978, ApJ, 224, 132  
 Cardelli J.A., Clayton G.C., Mathis J.S., 1989, ApJ, 345, 245  
 Conway J.E., 1999, NewAR, 43, 509  
 Conway J.E., Blanco P.R., 1995, ApJ, 449, L131  
 de Koff S. et al., 2000, ApJS, 129, 33  
 Dennett-Thorpe J., Bridle A.H., Laing R.A., Scheuer P.A.G., 1999, MNRAS, 304, 271  
 Dickey J.M., Lockman F.J., 1990, ARA&A, 28, 215  
 Ferrière K.M., 2001, RvMP, 73, 1031  
 Giovannini G., Cotton W.D., Feretti L., Lara L., Venturi T., 2001, ApJ, 552, 508  
 Gallimore J.F., Baum S.A., O’Dea C.P., Pedlar A., Brinks E., 1999, ApJ, 524, 684  
 Gupta Neeraj, Salter C.J., Saikia D.J., Ghosh T., Jeyakumar S., 2006, MNRAS, submitted (astro-ph/0605423)  
 Gupta Neeraj, Saikia D.J., 2006, MNRAS, in press (astro-ph/0605399)  
 Hamann F., 1997, ApJS, 109, 279  
 Isobe N., Tashiro M., Makishima K., Iyomoto N., Suzuki M., Murakami M.M., Mori M., Abe K., 2002, ApJ, 580, L111  
 Jackson N., Rawlings S., 1997, MNRAS, 286, 241  
 Kulkarni S.R., Heiles C., 1988, in Galactic and Extragalactic Radio Astronomy, ed. G. Verschuur & K. Kellerman (Heidelberg: Springer), 95  
 Lawrence C.R., Zucker J.R., Readhead A.C.S., Unwin S.C., Pearson T.J., Xu W., 1996, ApJS, 107, 541  
 Marchesini D., Capetti A., Celotti A., 2005, A&A, 433, 841  
 Morganti R., Oosterloo T.A., Tadhunter C.N., van Moorsel G., Killeen N., Wills K.A., 2001, MNRAS, 323, 331  
 Morganti R., Tadhunter C.N., Oosterloo T.A., 2005, A&A, 444, L9  
 Pihlström Y.M., Conway J.E., Vermeulen R.C., 2003, A&A, 404, 871  
 Spergel et al., 2003, ApJS, 148, 175  
 Tadhunter C., Wills K., Morganti R., Oosterloo T., Dickson R., 2001, MNRAS, 327, 227  
 Tadhunter C., Marconi A., Axon D., Wills K., Robinson T.G., Jackson N., 2003, MNRAS, 342, 861  
 Taylor G.B., 1996, ApJ, 470, 394  
 van Gorkom J.H., Knapp G.R., Ekers R.D., Ekers D.D., Laing R.A., Polk K.S., 1989, AJ, 97, 708  
 van Langevelde H.J., Pihlström Y.M., Conway J.E., Jaffe W., Schilizzi R.T., 2000, A&A, 354, 45  
 Vermeulen R.C. et al., 2003, A&A, 404, 861  
 Vermeulen R.C., Labiano A., Barthel P.D., Baum S.A., de Vries W.H., O’Dea C.P., 2006, A&A, 447, 489  
 Villar-Martín M., Tadhunter C., Morganti R., Axon D., Koekemoer A., 1999, MNRAS, 307, 24